

Improving wing aeroelastic characteristics using periodic design

Hossam T. Badran^{*1}, Mohammad Tawfik^{2a} and Hani M. Negm^{1b}

¹Aerospace Engineering Department, Cairo University, Giza, Egypt

²Aerospace Engineering, University of Science and Technology, Zewail City for Science and Technology, Giza, Egypt

(Received August 17, 2016, Revised October 21, 2016, Accepted February 11, 2016)

Abstract. Flutter is a dangerous phenomenon encountered in flexible structures subjected to aerodynamic forces. This includes aircraft, buildings and bridges. Flutter occurs as a result of interactions between aerodynamic, stiffness, and inertia forces on a structure. In an aircraft, as the speed of the flow increases, there may be a point at which the structural damping is insufficient to damp out the motion which is increasing due to aerodynamic energy being added to the structure. This vibration can cause structural failure, and therefore considering flutter characteristics is an essential part of designing an aircraft. Scientists and engineers studied flutter and developed theories and mathematical tools to analyze the phenomenon. Strip theory aerodynamics, beam structural models, unsteady lifting surface methods (e.g., Doublet-Lattice) and finite element models expanded analysis capabilities.

Periodic Structures have been in the focus of research for their useful characteristics and ability to attenuate vibration in frequency bands called “stop-bands”. A periodic structure consists of cells which differ in material or geometry. As vibration waves travel along the structure and face the cell boundaries, some waves pass and some are reflected back, which may cause destructive interference with the succeeding waves. This may reduce the vibration level of the structure, and hence improve its dynamic performance.

In this paper, for the first time, we analyze the flutter characteristics of a wing with a periodic change in its sandwich construction. The new technique preserves the external geometry of the wing structure and depends on changing the material of the sandwich core. The periodic analysis and the vibration response characteristics of the model are investigated using a finite element model for the wing. Previous studies investigating the dynamic bending response of a periodic sandwich beam in the absence of flow have shown promising results.

Keywords: vibration; flutter; wing; sandwich beam; finite elements; periodic structure; stop bands

1. Introduction and literature survey

Physical systems such as wings can be modelled as beams, whose study frequently results in partial differential equations which cannot be solved by an exact analytic solution. Two beam

*Corresponding author, Ph.D. Student, E-mail: htbadran@hotmail.com

^aAssociate Professor, E-mail: mohammad.tawfik@gmail.com

^bProfessor, E-mail: hnegm_cu@hotmail.com

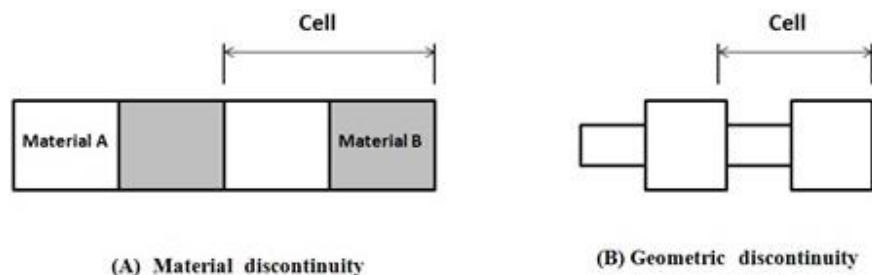


Fig. 1 Type of discontinuities

models are in common use in structural mechanics; namely, Euler-Bernoulli beam model and Timoshenko beam model. Crawley and De Luis (1987), developed analytical models of beams with piezoelectric actuators. These models illustrate the mechanics of Euler-Bernoulli beams with surface mounted actuators, and the analytical results have been verified by carrying out experiments. Chandrashekhara and Varadarajan (1997), presented a finite element model for a composite beam using a higher-order shear deformation theory. Aldraihem *et al.* (1997), developed laminated beam models using the two theories; namely, Euler-Bernoulli beam theory and Timoshenko beam theory. Here, the piezoelectric layers were used to control the vibration of a cantilever beam. Donthireddy and Chandrashekhara (1996), presented a new technique of modelling and shape control of composite beams with embedded piezoelectric actuators. A finite element model was developed for the dynamic analysis of Timoshenko beams by Thomas and Abbas (1975). Analytical formulation and closed form solutions for laminated composite beams with piezoelectric actuators based on Timoshenko beam theory were presented by Abramovich (1998). Manjunath and Bandyopadhyay (2005), discussed the vibration control of beams modelled using Timoshenko beam theory, and using different aspect ratios for the beam. Aldraihem and Khdeir (2000), propose analytical models and exact solutions for beams with shear and extension piezoelectric actuators, and the models were based on Timoshenko beam theory and higher-order beam theory (HOBT).

Zhang and Sun (1996), formulates an analytical model for a sandwich beam with a shear piezoelectric actuator that occupies the entire core. The model derivation was simplified by assuming that the face layers follow Euler-Bernoulli beam theory, whereas the core layer obeys Timoshenko beam theory, which will be adopted in the present work. There have been numerous finite element and analytical studies concerning the use of shear piezoelectric elements (PZT) as a core for sandwich structures. Benjeddou *et al.* (1999), derived a shear actuated beam finite element with the facings modelled as Euler-Bernoulli beams and the core modelled as a shear deformable Timoshenko beam. It was found that the shear-mode of actuation performs better on stiffer structures than its extensional counterpart.

In their paper, Mead and Parathan (1979) define a periodic structure as a structure that consists fundamentally of a number of dissimilar structural components (cells) that are joined together to form a continuous structure. This introduces sudden changes in the properties of the structure. There are two main types of discontinuities: (1) Geometric discontinuity and (2) Material discontinuity. Fig. 1 shows the two different types of discontinuities. The transfer matrix approach, in general, is based on developing a relation between the two ends of a structural element.

The real power of the transfer matrix approach comes when the structure can be divided into a set of substructures with a set of elements and nodes that are connected to another set on some

fictitious boundary inside the structure. Using the method of static condensation, the internal nodes/degrees of freedom of the substructure can be eliminated, thus reducing the size of the global matrices of the structure. When the set of equations of the substructure can be manipulated to collect the forces and displacements of one end of the substructure on one side of the equation, and relate them to those on the other end with a matrix relation, this matrix relation is called the transfer matrix of the structure. The transfer matrix of a substructure, other than being of reduced order, is then multiplied by that of the neighbouring structure, in contrast with the superposition method that is used in conventional numerical techniques. Thus, the matrix system that describes the dynamics of the structure becomes of significantly smaller size. The transfer matrix method becomes of even more appealing features when the substructures can be selected in a manner that they are all identical, thus, calculating the transfer matrix for one substructure is sufficient to describe the dynamics of the whole structure easily. In this section, we review the research works performed in the area of wave propagation in periodic structures. Ungar (1966) derived an expression that describes the steady state vibration of an infinite beam uniformly supported on impedances. Later, Gupta (1970), presented an analysis for periodically-supported beams that introduced the concepts of the cell and the associated transfer matrix. He presented the propagation and attenuation parameter plots which form the foundation for further studies of one-dimensional periodic structures. Faulkner and Hong (1985), presented a study of general mono-coupled periodic systems. Their study analysed the free vibration of spring-mass systems as well as point-supported beams using analytical and finite element methods. Mead and Yaman (1991), presented a study of the response of one-dimensional periodic structures subject to periodic loading. Their study involved generalization of the support condition to involve rotational and displacement springs as well as impedances. The effects of the excitation point as well as the elastic support characteristics on the pass and stop characteristics of the beam were presented. Langley (1996), presented the basic property of a symplectic matrix whose eigenvalues appear in pairs, one of which is the reciprocal of the other. This property of the transfer matrix introduces simplicity into the analysis; but unfortunately, introduces numerical instabilities in the numerical solution of structures with a large number of cells.

Flutter is defined as a dynamic instability of an elastic structure in a fluid flow, caused by positive feedback between the body's deflection and the forces exerted by the fluid flow. In a linear system, 'flutter point' is the point at which the structure is undergoing simple harmonic motion-zero net damping, and so any further decrease in the net damping will result in a self-oscillation and eventual failure. Georghiadis and Banerjee (1997) investigated the flutter behaviour of uniform composite wings using parametric study. The wing is idealized as a bending torsion (materially) coupled composite beam with cantilever end conditions for which the frequency equation and mode shapes in free vibration are presented in closed analytical form. Guo *et al.* (2003), presented an analytical study on optimization of a laminated composite wing structure for achieving a maximum flutter speed and a minimum weight without strength penalty. Attention has been paid mainly to the effect on flutter speed of the bending, torsion and, more importantly, the bending-torsional coupling rigidity, which is usually associated with asymmetric laminate lay-up. Kameyama and Fukunaga (2007), treated the flutter and divergence characteristics of composite plate wings with various sweep angles. The effect of laminate configuration on the flutter and divergence characteristics is investigated for composite plate wings. Guo (2007), presented an investigation into a minimum weight optimal design and aeroelastic tailoring of an aerobatic aircraft wing structure. Based on a minimum weight composite wing box model of adequate strength the investigation was focused on the aeroelastic tailoring of

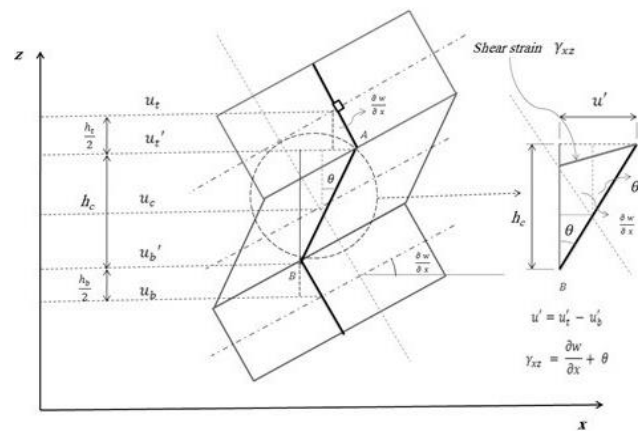


Fig. 2 Kinematics of sandwich wing

the wing box by employing the gradient-based deterministic optimization method.

2. Mathematical modeling of smart sandwiched wing

A sandwiched wing (piezo-laminated composite beam) is shown in Fig. 2. It consists of 3 layers; a piezo-patch with rigid foam sandwiched between two aluminium layers. All layers are supposed to be perfectly bonded, in plane-stress state, and having the same transverse displacement. The deformation of the face sheets obeys Euler-Bernoulli theory, while that of the core obeys Timoshenko theory.

2.1 Kinematics description

We will define all the mechanical quantities such as: displacements, strains and energies in terms of the transverse displacements (w) and longitudinal displacements of the top and bottom layers (u_t) and (u_b), respectively as shown in Fig. 2. The longitudinal displacements of the layers are linear with height, the top and bottom layers resist axial and bending loads only, and the core layer resists shear load in addition to axial and bending loads. All layers resist torsion load.

2.2 Strain-displacement relations

As shown in Fig. 2, the axial, transverse and shear displacements of the top, bottom and core layers can be written as

$$\begin{aligned}
 u_t(x) &= u_t' - \left(\frac{h_t}{2}\right) \frac{\partial w}{\partial x} \\
 u_b(x) &= u_b' + \left(\frac{h_b}{2}\right) \frac{\partial w}{\partial x} \\
 u_c(x) &= \frac{u_t + u_b}{2} + \left(\frac{A_2}{2}\right) \frac{\partial w}{\partial x}
 \end{aligned} \tag{1}$$

Table 1 Natural frequencies (Hz) of shear sensory actuated cantilever wing

	1 st	2 nd	3 rd	4 th	5 th
Finite element Benjeddou <i>et al.</i> (1999)	985	3912	8305	17273	25980
Finite element (short circuited)	985	3911	8297	17226	25849
Finite element (open circuited)	988	3924	8352	17406	26273

Then, the strain of different layers and the rotation of core layer due to axial and bending actions are obtained by differentiating the above displacements with respect to (x) . The core layer the shear strain and rotation will be described according to Fig. 2 as having these values: $\gamma_{xz}=(u_t-u_b)/h_c+(A_3/h_c)\partial w/\partial x$ and $\theta(x)=(u_t-u_b)/h_c+(A_1/h_c)\partial w/\partial x$ respectively. Where, subscripts (t), (b) and (c) denote top, bottom and core layers respectively. A_i are defined in Appendix 1.

3. Constitutive equations

The three dimensional linear constitutive equations of orthotropic PZT ceramic core of the shear mode have the following form, Trindade *et al.* (1999).

$$\begin{Bmatrix} \sigma_x^c \\ \tau_{zx} \\ D_3 \end{Bmatrix} = \begin{bmatrix} Q_{33} & 0 & 0 \\ 0 & Q_{55} & -e_{15} \\ 0 & e_{15} & \epsilon_1 \end{bmatrix} \begin{Bmatrix} \epsilon_x^c \\ \gamma_{zx} \\ E_3 \end{Bmatrix} \quad (2)$$

The linear constitutive equations of face layers have the form

$$\{\sigma_k\} = [E_k] \times \{\epsilon_k\} \quad (3)$$

The linear constitutive equation of the electric potential applied through the core layer has the following form

$$\phi_c = \bar{\phi}_c + \frac{V_c}{h_c} z \quad (4)$$

The electric potential in the core is shown to be linear in the thickness direction.

Since $(E_3 = -\partial\phi_c/\partial z)$, so Eq. (4) reduces to

$$E_3 = -\frac{V_c}{h_c} \quad (5)$$

4. Development of equations of motion

The dynamic equations of motion in this investigation are developed using Hamilton's principle, Reddy (2002).

$$\delta\Pi = \int_{t_1}^{t_2} (\delta T - \delta U + \delta W) dt = 0 \quad (6)$$

Where, $\delta\Pi$: Total system energy, δT : Kinetic energy, δU : Strain energy and δW : Work done

by external forces. By taking the first variation for strain energy, kinetic energy and external work, then integrating by parts with respect to time (t_1 and t_2 are arbitrary) we get the weak form of Hamilton's principle, which is used for deriving the finite element equations of the system. The variation of the element strain energy with PZT core is as following

$$\begin{aligned} \delta U_{to}^p = & \int_0^L \delta(u_t')B1(u_t') + \delta(u_b')B2(u_b') + \delta(w'')B3(w'') + \delta(u_t')(B4)(u_b') + \\ & \delta(u_b')B4(u_t') + \delta(u_t')B5(w'') + \delta(w'')B5(u_t') + \delta(u_b')B6(w'') + \delta(w'')B6(u_b') + \\ & \delta(u_t)B7 \delta(u_t) + \delta(u_b)B7(u_b) + \delta(w')B8(w') - \delta(u_t)B9(u_b) - \delta(u_b)B9(u_t) - \\ & \delta(u_b)B10(w') - \delta(w')B10(u_b) + \delta(u_t)B10(w') + \delta(w')B10(u_t) + \delta(V_c)B11(u_t) + \\ & \delta(u_t)B11(V_c) - \delta(V_c)B11(u_b) - \delta(u_b)B11(V_c) + \delta(V_c)B12(w') + \delta(w')B12(V_c) - \\ & \delta(V_c)B13(V_c)dx \end{aligned} \quad (7)$$

Where, B's are defined in Appendix 1. For Foam core the total strain energy is the same of PZT core except for deleting the terms containing the electrical-mechanical terms B11, B12 and B13, and replacing them by the B's by C's which are defined in Appendix 1.

The variation of the system total kinetic energy with Ceramic core is as following

$$\begin{aligned} \delta T_{to}^p = & \int_0^L \delta(\dot{u}_t)D1(\dot{u}_t) + \delta(\dot{u}_b)D2(\dot{u}_b) + \delta(\dot{w}')D3(\dot{w}') + \delta(\dot{u}_t)D4(\dot{u}_b) + \\ & \delta(\dot{u}_b)D4(\dot{u}_t) + \delta(\dot{u}_t)D5(\dot{w}') + \delta(\dot{w}')D5(\dot{u}_t) + \delta(\dot{u}_b)D6(\dot{w}') + \delta(\dot{w}')D6(\dot{u}_b) + \\ & \delta(\dot{w}')D7(\dot{w}')dx \end{aligned} \quad (8)$$

Where, D's are defined in Appendix 1. For Foam Core the total kinetic energy is the same as for PZT core with replacing the D's by H's which are defined in Appendix 1.

The variation of the total external work done on the system (δW_t)

$$\delta W_t = \int_V \{\delta q\}^T \{f_b\} dV + \int_A \{\delta q\}^T \{f_s\} dA + \{\delta q\}^T \{f_p\} - \int_{A_e} \rho \{\delta \Phi\} dA_e \quad (9)$$

Where: $\{f_b\}$, $\{f_s\}$, $\{f_p\}$ and $\{q\}$ are the external body, surface, point forces and nodal displacements respectively. ρ and $\{\delta \Phi\}$ are surface charge and electric potential respectively. By substituting Eqs. (7) to (9) into Eq. (6) we get the weak form of Hamilton's principle which we use in the finite element analysis.

5. Finite element formulation

The weak form of Hamilton' Principle derived in Eq. (6) will now be used to develop the finite element model of the suggested three-layer sandwich wing with PZT Ceramic-Foam core. Lagrange linear shape functions are used for axial displacement field u_t , u_b and electrical potential V_c , which are C^0 -type continuous, while Hermitian shape functions are used for transverse displacement w , which are C^1 -type. This means that the deflection w and slope ($\partial w/\partial x$) are continuous between two neighbouring elements. The proposed model is a three-node finite beam element for mechanical and electrical degrees of freedom; each node has four mechanical degrees of freedom and one electrical degree of freedom. The shape functions of the mechanical and electrical variables are similar to those in Badran (2008a). The element total stiffness matrix with PZT ceramic core will be derived according to Eq. (7) by splitting it into four parts: $U_{to} = \delta U_m + \delta U_{me} + \delta U_{em} + \delta U_e$, where δU_m , δU_{me} , δU_{em} and δU_e the mechanical, piezoelectric coupling and dielectric terms of δU_{to}^p respectively, which have the following values: $\delta U_{me}^a = \bar{\delta}_m^T [K_m] \bar{\delta}_m$, $\delta U_{me}^a = \bar{\delta}_m^T [K_{me}^a] \bar{\delta}_e$, $U_{em}^a = \bar{\delta}_e^T [K_{em}^a] \bar{\delta}_m$ and $\delta U_e^a = \bar{\delta}_e^T [K_e] \bar{\delta}_e$.

The element total mass matrix will be derived according to Eq. (8) as: $\delta T_{to}^p = \delta \dot{q}^T [M_p] \dot{q}$. The mechanical and electrical applied force are introduced according to Eq. (9) giving of the variation of external work. The element stiffness matrices, mass matrix and force vector of the adaptive sandwich wing are given in Appendix 2. By substituting the mass, stiffness and force vector in Eq. (6), the equations of motion can be written as

$$[M]\{\ddot{\delta}_m\} + [K_m]\{\delta_m\} + [K_{me}]\{\delta_e\} = \{F_m\} \quad (10)$$

$$[K_{em}]\{\delta_m\} + [K_e]\{\delta_e\} = \{F_e\} \quad (11)$$

Where: δ_m and δ_e are the global nodal generalized displacement and electrical coordinates respectively. By applying electrical boundary conditions such as short-circuited or open-circuited boundary conditions, the coupled governing equation set can be solved explicitly. For voltage driven electrodes (short circuit) where the electric potential δ_e is specified, Eq. (10) results in

$$[M]\{\ddot{\delta}_m\} + [K_m]\{\delta_m\} = \{F_m\} - [K_{me}^a]\{\delta_e\} \quad (12)$$

The second term on the right hand side $[K_{me}^a] \delta_e$ represents the equivalent PZT ceramic loads. The mechanical displacement can be solved from this equation and consequently substituted in Eq. (11) to calculate the electric charges. It can be observed that for short circuited electrodes where $\{\delta_e\} = 0$, Eq. (12) is identical to those where no PZT ceramic electromechanical coupling exists. Then, one ends up with the eigenvalue problem

$$([K_m] - \omega^2[M])\{\delta_m\} = 0 \quad (13)$$

Eq. (13) shows that the natural frequencies and mode shapes of the short-circuited system are the same as those of non-PZT ceramic system.

For open circuited electrodes, the electric charge is zero ($\{F_e\} = 0$), hence, $\{\delta_e\}$ can be obtained from Eq. (11) as: $\{\delta_e\} = -[K_e]^{-1}[K_{em}]\{\delta_m\}$.

By substituting in Eq. (10), we get

$$[M]\{\ddot{\delta}_m\} + ([K_m] - [K_{me}][K_e]^{-1}[K_{em}])\{\delta_m\} = \{F_m\} \quad (14)$$

We find that PZT ceramic electromechanical coupling increases the overall stiffness of the system if the electrodes are open, because of $[K_e]^{-1}$ is negative. In this case the natural frequencies are greater than the case when the coupling is neglected.

A computer code has been developed to calculate the natural frequency in short and open-circuited cases as shown in Table 1. Table 1 compares the calculated values of the first five natural frequencies of the sandwich cantilever beam with (PZT-Foam) core with the results of Benjeddou (1999). The results validate the correctness of the equations, matrices and computer programs of the suggested three-node sandwich beam finite element model using 3-elements, and show that the accuracies of the two models are almost identical. Also, they show that the natural frequencies improve with open circuited condition by attaining higher values.

6. Periodic analysis

Periodic structures can be modelled like any ordinary structure, however, studying the behaviour of one cell is sufficient to determine the stop and pass bands of the complete structure independent of the number of cells. In the present work, the frequency domain is classified into

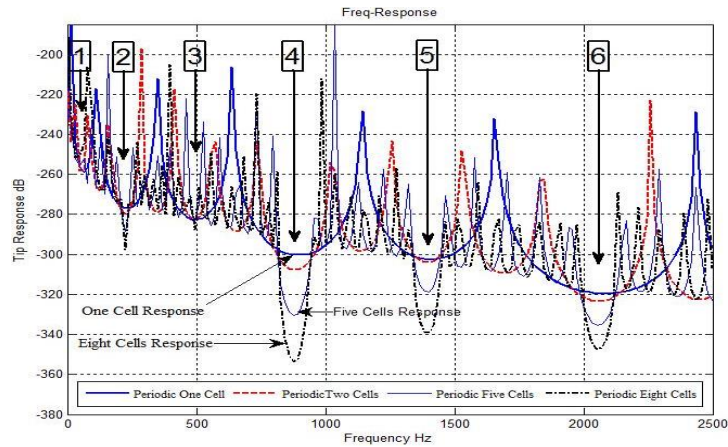


Fig. 3 Effect of number of cells on frequency response

pass-bands, i.e., frequencies for which excited surface waves get through the periodic piezoelectric device, and stop-bands, i.e., frequencies which cannot pass through. Therefore, the piezoelectric device can be used for frequency filtering. There are two approaches for the analysis of the periodic characteristics of a beam: the forward approach and the reverse approach, as introduced in Badran *et al.* (2008b). A code was developed for a periodic sandwich beam with a Ceramic PZT (ignoring the piezoelectricity effect) and Foam core, in order to study the effect of core structural periodicity on attenuating the vibration of beams. Fig. 3 shows the results obtained by the developed code for beams divided into different numbers of cells. The general specifications of the beam under study are mentioned in Badran (2008a). It is found that the response of the periodic sandwich beam is significantly improved through reduction of the vibration amplitudes at the positions of the stop bands. Fig. 3 shows the frequency response of a periodic sandwich beam divided into eight cells, five cells, two cells and one cell for a frequency range 0-2500 Hz. It is seen from the Fig. 3 that the frequency response of the periodic sandwich beam has been significantly improved through reduction of the vibration amplitudes at the positions of the stop bands.

7. Wing flutter

The equations of motion are derived using energy methods by applying Hamilton's principle, which offers a convenient formulation for any number of discrete generalized or physical coordinates.

The equation of motion has the form

$$[M]\{\ddot{q}\} + [K]\{q\} = \{F\} \quad (15)$$

Where, $\{q\}$ is the coordinate vector containing both the twisting and bending degrees of freedom: $\{q\}^T = \{w_1 \ \theta_1 \ \alpha_1 \ \dots \ w_N \ \theta_N \ \alpha_N\}^T$. For flutter analysis, a harmonic motion with oscillation frequency ω is assumed, so the governing equation becomes

$$(-\omega^2[M] + [K])\{\bar{q}\} = \{\bar{F}\} \quad (16)$$

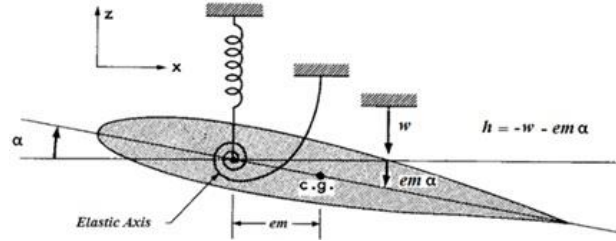


Fig. 4 Two-DOF bending and torsion airfoil model

Where, \bar{q} is the amplitude of the deformation vector, \bar{F} is the amplitude of the load vector, $[M]$ is the global mass matrix, and $[K]$ is the global stiffness matrix. In Eq. (16) the right hand side is derived using the Aerodynamic model, and the left hand side is derived using the Structural model. The natural frequency (ω) occurs in a free vibration case where the system acts independent of the external forces.

7.1 Structural model

Double symmetry of the structure cross section leads to decoupling of the bending and torsional motions. The loss of cross sectional symmetry leads to a coupling effect between the bending and torsional motions due to an offset between the center of gravity and the shear center; a distance referred to as inertial eccentricity. The resulting equations of motion are inertially coupled, but elastically uncoupled.

The coupled elastic potential energy (U) is given as

$$U = \frac{1}{2} EI \int_0^L \left(\frac{\partial^2 w}{\partial y^2} \right)^2 dy + \frac{1}{2} GJ \int_0^L \left(\frac{\partial \theta}{\partial y} \right)^2 dy \tag{17}$$

The coupled kinetic energy (T) is given as

$$T = \frac{1}{2} \int_{chord} \left(\frac{\partial h}{\partial t} \right)^2 dm \tag{18}$$

By referring to Fig. 4, $h = -w - em \alpha$

Substituting (h) in Eq. (18) it can be shown that, Guertin ML (2012)

$$T = \frac{1}{2} (\mu) \int_0^L (\dot{w})^2 dx + \frac{1}{2} (2 S_\alpha) \int_0^L (\dot{w})(\dot{\theta}) dx + \frac{1}{2} (I_\alpha) \int_0^L (\dot{\theta})^2 dx \tag{19}$$

Where, EI : bending rigidity, GJ : torsion rigidity, ρ_m : material density, A : cross section area, I_o : polar moment of inertia, e_m : inertial eccentricity (offset of center of gravity from the elastic center), μ : mass per unit length ($\rho_m A$), b : half chord, a : offset of the mid chord from the elastic axis (non-dimensional), S_α : static mass moment per unit span about the axis $x=ba$, and equals (μe_m), and I_α : mass moment of inertia per unit length, and equals ($\rho_m I_o$). By calculating the potential and kinetic energies of the structural model and applying Hamilton's principle, then using finite elements having two-nodes and three degrees of freedom per node (torsion, transverse displacement and rotation), we get the system of equations representing an eigen value problem. Solving these equations, we get the natural frequencies and mode shapes due to bending and torsion.

7.2 Aerodynamic model

The Theodorsen's 2-D thin aerofoil theory will be used to evaluate the unsteady aerodynamic forces and moments per unit L_i and M_i span using thin aerofoil theory with a Theodorsen's lift deficiency function, Bisplinghoff *et al.* (1996).

These can be cast in a matrix form as follows

$$\begin{Bmatrix} L_i \\ M_i \end{Bmatrix} = \omega^2 \begin{bmatrix} L_{1i} & L_{2i} \\ M_{1i} & M_{2i} \end{bmatrix} \begin{Bmatrix} h_i \\ \alpha_i \end{Bmatrix} \quad (20)$$

Where, $L_{1i} = \pi \rho b_i^2 [L_h^i]$, $L_{2i} = \pi \rho b_i^3 [L_\alpha^i - L_h^i (a + \frac{1}{2})]$, $M_{1i} = \pi \rho b_i^3 [M_h^i - L_h^i (a + \frac{1}{2})]$, $M_{2i} = \pi \rho b_i^4 [M_\alpha^i - (L_\alpha^i + M_h^i) (a + \frac{1}{2}) + L_h^i (a + \frac{1}{2})^2]$, ρ : air density, b_i : semi-chord, h : amplitude of the vertical displacement, α_i : amplitude of the twisting angle, a : distance between the elastic axis and the mid-chord point as a fraction of the semi-chord, U : forward flight speed, L_h^i , L_α^i , M_h^i and M_α^i are aerodynamic lift and moment coefficients, k : reduced frequency, and equals: $k = \frac{\omega b_i}{U}$, ω : frequency of oscillation (flutter frequency).

The external virtual work done by the aerodynamic forces per unit span at an aerodynamic node can be written as follows

$$W_i = \delta h_i (L_i) + \delta \alpha_i (M_i) \quad (21)$$

This can be written in the form

$$F_i = \Delta y_i [\delta h_i \quad \delta \alpha_i] \begin{Bmatrix} L_i \\ M_i \end{Bmatrix} \quad (22)$$

Using two-node beam elements, the elastic axis deformation can be interpolated from the deformation of the two end nodes by using first order polynomials for the torsional twist angle and third order polynomials for the transverse displacement as follows

$$u_e = \begin{Bmatrix} h_i \\ \alpha_i \end{Bmatrix} = [\mathbf{N}] \{q\}_e \quad (23)$$

Where $[\mathbf{N}]$, is the shape function vector, $\{q\}_e$ is the end nodes deformation vector in the wing local axes. Substituting Eq. (23) into Eq. (20) and then into Eq. (22) we get

$$F_i = \omega^2 \{\delta q\}_e^T [\mathbf{N}]^T [\mathbf{F}_i] [\mathbf{N}] \{q\}_e \quad (24)$$

$$\text{Where, } [\mathbf{F}_i] = \Delta y_i \begin{bmatrix} L_{1i} & L_{2i} \\ M_{1i} & M_{2i} \end{bmatrix}$$

The elemental unsteady aerodynamic matrix can be obtained by summing all the external virtual work done at all the aerodynamic nodes at the middle of the structural element

$$[A]_e = [\mathbf{N}]_{6 \times 2n_a}^T [\mathbf{F}_i]_{2n_a \times 2n_a} [\mathbf{N}]_{2n_a \times 6} \Big|_{at \ x=\frac{l}{2}} \quad (25)$$

Where, n_a is the number of the aerodynamic nodes taken over a single element.

Table 2 GOLAND wing frequencies

	Present work	Banerjee (1999)
1 st Bending frequency (rad/sec)	49.4922	49.6
1 st Torsion frequency (rad/sec)	96.049	97.0

Table 3 GOLAND wing flutter speed (mph)

	No of Elements				Flutter speed (mph)	Reference
	2	3	5	10		
Flutter Speed (mph)	394.93	385.24	380.97	379.32	385.00 Assumed odes	Bisplinghoff <i>et al.</i> (1996)

So, the equation of the dynamic system after assembling all matrices can be written as

$$(-\omega^2[M] + [A]) + [K]\{\bar{q}\} = 0 \tag{26}$$

The flutter analysis can be performed using the familiar V-g method, Bisplinghoff *et al.* (1996). The structural damping coefficient (*g*) is introduced in the equations of motion, representing the amount of damping that must be added to the structure to attain neutral stability at the given velocity. Negative values of structural damping (*g*) indicate that the structure is stable, while positive values indicate instability. Flutter occurs when the structural damping coefficient (*g*) equals the actual damping of the structure, which is nearly zero, Hollowell and Dugundji (1984). Substituting in Eq. (26), the following eigenvalue problem is obtained

$$([K]^{-1}([M] + [A]) - \left(\frac{1+gi}{\omega^2}\right)[I])\{\bar{q}\} = 0 \tag{27}$$

The above equation can be solved as

$$([K]^{-1}([M] + [A]))\{\bar{q}\} = \left(\frac{1+gi}{\omega^2}\right)[I]\{\bar{q}\} \tag{28}$$

$$([K]^{-1}([M] + [A]))\{\bar{q}\} = (Z[I])\{\bar{q}\}$$

The above equation can be solved for the complex eigenvalues (*Z*) for several values of the reduced frequency by equating both the imaginary and real parts on both sides. Then we can calculate the flutter frequency (ω_f), damping (*g*) and flutter speed (U_f) as follows

$$\omega_f = \sqrt{\frac{1}{Z(Re)}}, \eta = \frac{Z(Im)}{Z(Re)}, U_f = \frac{\omega_f b}{k} \tag{29}$$

The values of (*g*) and (ω) are plotted vs. (U_f), and the ω value at *g*=0 represents the flutter frequency (ω_f). A computer code was developed for the smart periodic wing. The finite element model consists of two models: a structural model, which is a geometric model of the wing, and an aerodynamic model, which calculates the unsteady aerodynamic loads acting on the wing.

7.3 Flutter numerical validation

The Goland wing is a low-aspect-ratio prismatic metallic wing, which has been extensively used for validation in the literature. It is a structurally uncoupled wing with some inertial coupling. The

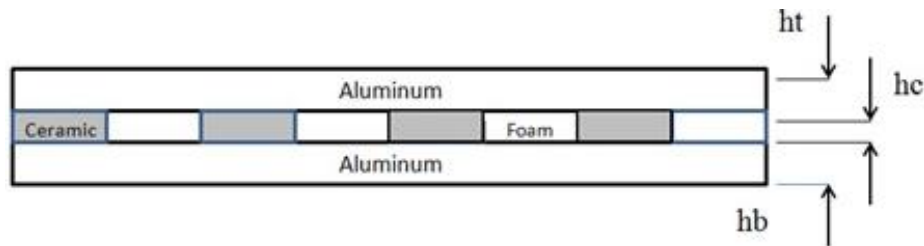


Fig. 5 Proposed periodic wing

Goland wing characteristics are given in Goland and Buffalo (1945). Table 2 compares the calculated fundamental bending and torsion frequencies for the Goland wing using the present model with those given in Banerjee (1999). Table 3 gives the calculated flutter speed and frequency for the wing using different numbers of elements, and compares them with those of Bisplinghoff *et al.* (1996). It is seen that dividing the wing into 3 finite elements gives sufficient accuracy.

8. Improvement of wing flutter using periodic design

We use periodic design to improve the flutter speed of wing. This periodic wing is modelled as a sandwich beam with three layers: top, bottom and core layers. The top and bottom layers are made of aluminium alloy and the core is made of two different materials side by side; PZT ceramic material and foam as shown in Fig. 5. As the wave propagates through the blade core and faces a cell boundary, part of the wave is reflected and another part propagates into the next cell. The reflected part of the wave interferes with the incident wave. The interference between the incident and reflected waves results in a destructive action at some frequency bands. In the frequency band where destructive interference occurs, there is a reduced vibration level. This band is what we call Stop-Band. Other frequency bands are called Pass-bands. The Stop bands are the principal cause for using periodic design to improve the wings flutter characteristics. Having verified the computer code in section 6 for periodic structural analysis, and in section 7 for calculating the flutter speed for a standard wing, we now combine these codes to study the effect of periodicity on the flutter speed of the wing.

8.1 The proposed periodic wing model

The proposed wing characteristics are as follows: Half span 322 in (8.1788 m), Chord 20.76 in (0.5273 m), Wing thickness 0.036 m, Wing aspect ratio 14.79. The material properties for Aluminum are: Density $\rho=2690 \text{ Kg/m}^3$, Modulus of Elasticity $E=70.3 \times 10^9 \text{ N/m}^2$ and Modulus of Rigidity $G=25.9 \times 10^9 \text{ N/m}^2$. The material properties for Ceramic PZT are: $\rho=7750 \text{ Kg/m}^3$, $E=86.8 \times 10^9 \text{ N/m}^2$ and $G=23 \times 10^9 \text{ N/m}^2$. The material properties for FOAM are: $\rho=32 \text{ Kg/m}^3$, $E=35.3 \times 10^6 \text{ N/m}^2$ and $G=12 \times 10^6 \text{ N/m}^2$.

Now we study the effect of periodic design on the flutter speed of a wing made of aluminium of three layers, top, core and bottom, all made of aluminium. In order to make a fair comparison between the solid and periodic core models we use the same outer dimensions, total mass, and flight conditions.

8.2 Flutter speed of solid core wing

It has been found by applying the proposed model that the flutter speed of the solid core wing at an altitude of 1000 m is 47.5 m/sec.

8.3 Flutter speed of wing with periodic core

The proposed periodic core is a sandwich wing with three layers: the top and bottom layers are made of Aluminium, and the core is periodic PZT Ceramic-Foam side by side. We choose the main geometry of the periodic model to be similar to the solid model, with the same total thickness and total length of the wing. In this case the mass is 458.4 Kg compared to 399.6 Kg for the solid blade. So we will change the thickness of the layers to have a thickness ratio (h_p/h_t) of 0.5 and the lengths of the cells to have a cell length ratio (L_p/L_t) of 0.5. These values reduce the mass of the proposed periodic core model to that of the solid model.

The flutter speed of the sandwich wing has been calculated at the same altitude using the proposed model for 6 pairs of periodic cells. The results show that the flutter speed has increased to 51.53 m/sec, which represents an improvement of 8.5%.

9. Conclusions

Aeroelastic performance of aircraft wing structures is of extreme importance. An aircraft wing must not experience flutter instability at all possible speeds. Periodic design of structures has proved to be useful in improving the dynamic performance in the absence of flow. A periodic structure is composed of repeated groups of cells of different material or geometry. This causes destructive interference between the waves travelling along the structures, and hence reduces its vibration level.

In this paper a periodic wing design is suggested as a beam composed of a core sandwiched between two aluminium faces layers. The beam is divided into cells in which the core is made of piezo ceramic or foam patches in an alternate order. The flutter speed is calculated for such a periodic sandwich wing using finite element method in the structural analysis, and Theodorsen's 2-D thin aerofoil theory with a lift deficiency function for the unsteady aerodynamic analysis, assuming incompressible flow conditions. The wing flutter speed is calculated using V-g method for 6 pairs of periodic cells, and compared with that of the nonperiodic solid wing having the same mass. Results of the calculations show that the flutter speed of the periodic wing is higher than that of the nonperiodic wing having the same mass.

References

- Abramovich, H. (1998), "Deflection control of laminated composite beam with piezoceramic layers-closed form solutions", *Compos. Struct.*, **43**(3), 217-231.
- Aldraihem, O.J. and Khdeir, A.A. (2000), "Smart beams with extension and thickness-shear piezoelectric actuators", *Smart Mater. Struct.*, **9**(1), 1-9.
- Aldraihem, O.J., Wetherhold, R.C. and Singh, T. (1997), "Distributed control of laminated beams: Timoshenko vs. Euler-Bernoulli theory", *J. Intell. Mater. Syst. Struct.*, **8**(2), 149-157.
- Badran, H.T. (2008a), "Vibration attenuation of periodic sandwich beams", M.S. Dissertation, Cairo

- University, Egypt.
- Badran, H.T., Tawfik, M. and Negm, H.M. (2008b), "Vibration characteristics of periodic sandwich beams", *Proceedings of the 13th International Conference on Applied Mechanics and Mechanical Engineering*, Cairo, Egypt.
- Bannerjee, J.R. (1999), "Explicit frequency equation and mode shapes of a cantilever beam coupled in bending and torsion", *J. Sound Vibr.*, **224**(2), 267-281.
- Benjeddou, A., Trindade, M.A. and Ohayon, R. (1999), "New shear actuated smart structure beam finite element", *Am. Inst. Aeronaut. Astronaut. J.*, **37**(3), 378-383.
- Bisplinghoff, R.L., Ashley, H. and Halfman, R.L. (1996), *Aeroelasticity*, Dover Publishers, New York, U.S.A.
- Chandrashekhara, K. and Varadarajan, S. (1997), "Adaptive shape control of composite beams with piezoelectric actuators", *J. Intell. Mater. Syst. Struct.*, **8**(2), 112-124.
- Crawley, E.F. and De Luis, J. (1987), "Use of piezoelectric actuators as elements of intelligent structures", *Am. Inst. Aeronaut. Astronaut. J.*, **25**(10), 1373-1385.
- Daniel, M.D., Carlos, E.S., Jun, S.O. and Roberto, G.A. (2010), "Aeroelastic tailoring of composite plates through eigenvalues optimization", *Assoc. Argent. Mecán. Comput.*, **XXIX**, 609-623.
- Donthireddy, P. and Chandrashekhara, K. (1996), "Modelling and shape control of composite beam with embedded piezoelectric actuators", *Compos. Struct.*, **35**(2), 237-244.
- Faulkner, M.G. and Hong, D.P. (1985), "Free vibration of mono-coupled periodic system", *J. Sound Vibr.*, **99**(1), 29-42.
- Georghiades, G.A. and Banerjee, J.R. (1997), "Flutter prediction for composite wings using parametric studies", *Am. Inst. Aeronaut. Astronaut. J.*, **35**(4), 746-748.
- Goland, M. and Buffalo, N.Y. (1945), "The flutter of a uniform cantilever wing", *J. Appl. Mech.*, **12**(4), 197-208.
- Guertin, M.L. (2012), "The application of finite element methods to aeroelastic lifting surface flutter", M.S. Dissertation, Rice University, Houston, Texas, U.S.A.
- Guo, S.J. (2007), "Aeroelastic optimization of an aerobatic aircraft wing structure", *Aerosp. Sci. Technol.*, **11**(5), 396-404.
- Guo, S.J., Bannerjee, J.R. and Cheung, C.W. (2003), "The effect of laminate lay-up on the flutter speed of composite wings", *J. Aerosp. Eng.*, **207**(3), 115-122.
- Gupta, G.S. (1970), "Natural flexural waves and the normal modes of periodically-supported beams and plates", *J. Sound Vibr.*, **13**(1), 89-101.
- Hollowell, S.J. and Dugundji, J. (1984), "Aeroelastic flutter and divergence stiffness coupled, graphite/epoxy cantilevered plates", *J. Aircr.*, **21**(1), 69-76.
- Kameyama, M. and Fukunaga, H. (2007), "Optimum design of composite plate wings for aeroelastic characteristics using lamination parameters", *Comput. Struct.*, **85**(3-4), 213-224.
- Langley, R.S. (1996), "A transfer matrix analysis of the energetics of structural wave motion and harmonic vibration", *Proceedings of the Royal Society A: Mathematical, Physical and Engineering Sciences*, **452**, 1631-1648.
- Majid, D.L. and Basri, S. (2008), "LCO flutter of cantilevered woven 10 glass/epoxy laminate in subsonic flow", *Acta Mech. Sinica.*, **24**(1), 107-110.
- Manjunath, T.C. and Bandyopadhyay, B. (2005), "Modelling and fast output sampling feedback control of a smart Timoshenko cantilever beam", *J. Smart Struct. Syst.*, **1**(3), 283-308.
- Mead, D.J. (1996), "Wave propagation in continuous periodic structures: Research contributions from Southampton, 1964-1995", *J. Sound Vibr.*, **190**(3), 495-524.
- Mead, D.J. and Parathan, S. (1979), "Free wave propagation in two dimensional periodic plates", *J. Sound Vibr.*, **64**(3), 325-348.
- Mead, D.J. and Yaman, Y. (1991), "The response of infinite periodic beams to point harmonic forces: A flexural wave analysis", *J. Sound Vibr.*, **144**(3), 507-530.
- Reddy, J.N. (2002), *Energy Principles and Variational Methods in Applied Mechanics*, John Willy & Sons, New Jersey, U.S.A.

- Thomas, J. and Abbas, B.A. (1975), "Finite element methods for dynamic analysis of Timoshenko beam", *J. Sound Vibr.*, **41**, 291-299.
- Trindade, M.A., Benjeddou, A. and Ohayon, R. (1999), "Parametric analysis of the vibration control of sandwich beams through shear-based piezoelectric actuation", *J. Intell. Mater. Syst. Struct.*, **10**(5), 377-385.
- Ungar, E.E. (1966), "Steady-state response of one-dimensional periodic flexural systems", *J. Acoust. Soc. Am.*, **39**(5), 887-894.
- Zhang, X. and Sun, C. (1996), "Formulation of an adaptive sandwich beam", *Smart Mater. Struct.*, **5**(6), 814-823.

EC

Appendix 1

$$B_1 = \left(\frac{Q_{33}^c I_c}{h_c^2} + \frac{Q_{33}^c A_c}{4} + Q_{11}^t A_t \right),$$

$$B_2 = \left(\frac{Q_{33}^c I_c}{h_c^2} + \frac{Q_{33}^c A_c}{4} + Q_{11}^b A_b \right)$$

$$B_3 = \left(\frac{Q_{33}^c I_c (A1)^2}{h_c^2} + \frac{Q_{33}^c A_c (A2)^2}{4} + Q_{11}^t I_t + Q_{11}^b I_b \right)$$

$$B_4 = \left(\frac{Q_{33}^c (A_c)}{4} - \frac{Q_{33}^c I_c}{h_c^2} \right),$$

$$B_5 = \left(\frac{Q_{33}^c (A_c) (A2)}{4} + \frac{Q_{33}^c I_c (A1)}{h_c^2} \right)$$

$$B_6 = \left(\frac{Q_{33}^c A_c A2}{4} - \frac{Q_{33}^c I_c A1}{h_c^2} \right), B_7 = \left(\frac{K_s Q_{55} A_c}{h_c^2} \right)$$

$$B_8 = \left(\frac{K_s Q_{55} A_c (A3)^2}{h_c^2} \right), B_9 = \left(\frac{K_s Q_{55} A_c}{h_c^2} \right)$$

$$B_{10} = \left(\frac{K_s Q_{55} A_c (A3)}{h_c^2} \right), B_{11} = \left(\frac{e_{15} A_c}{h_c^2} \right)$$

$$B_{12} = \left(\frac{e_{15} A_c (A3)}{h_c^2} \right), B_{13} = \left(\frac{\epsilon_1 A_c}{h_c^2} \right)$$

$$C_1 = \left(\frac{E_f I_f}{h_c^2} + \frac{E_f A_f}{4} + Q_{11}^t A_t \right)$$

$$C_2 = \left(\frac{E_f I_f}{h_c^2} + \frac{E_f A_f}{4} + Q_{11}^b A_b \right)$$

$$C_3 = \left(\frac{E_f I_f (A1)^2}{h_c^2} + \frac{E_f A_f (A2)^2}{4} + Q_{11}^t I_t + Q_{11}^b I_b \right)$$

$$C_4 = \left(\frac{E_f A_f}{4} - \frac{E_f I_f}{h_c^2} \right),$$

$$C_5 = \left(\frac{E_f A_f (A2)}{4} + \frac{E_f I_f (A1)}{h_c^2} \right),$$

$$C_6 = \left(\frac{E_f A_f (A1)}{4} - \frac{E_f I_f (A2)}{h_c^2} \right),$$

$$C_7 = \left(\frac{K_s G_f A_f}{h_c^2} \right),$$

$$C_8 = \left(\frac{K_s G_f A_f (A3)^2}{h_c^2} \right),$$

$$C_9 = \left(\frac{K_s G_f A_f}{h_c^2} \right), \text{ and}$$

$$C_{10} = \left(\frac{K_s G_f A_f (A3)}{h_c^2} \right).$$

$$D_1 = \left(\frac{\rho_c A_c}{4} + \frac{\rho_c I_c}{h_c^2} + \rho_t A_t \right),$$

$$D_2 = \left(\frac{\rho_c A_c}{4} + \frac{\rho_c I_c}{h_c^2} + \rho_b A_b \right),$$

$$D_3 = \left(\frac{\rho_c A_c (A2)^2}{4} + \frac{\rho_c I_c (A1)^2}{h_c^2} + \rho_t I_t + \rho_b I_b \right),$$

$$D_4 = \left(\frac{\rho_c A_c}{4} - \frac{\rho_c I_c}{h_c^2} \right),$$

$$D_5 = \left(\frac{\rho_c A_c (A2)}{4} + \frac{\rho_c I_c (A1)}{h_c^2} \right),$$

$$D_6 = \left(\frac{\rho_c A_c (A2)}{4} - \frac{\rho_c I_c (A1)}{h_c^2} \right)$$

$$D_7 = (\rho_t A_t + \rho_c A_c + \rho_b A_b)$$

$$H_1 = \left(\frac{\rho_f A_f}{4} + \frac{\rho_f I_f}{h_f^2} + \rho_t A_t \right),$$

$$H_2 = \left(\frac{\rho_f A_f}{4} + \frac{\rho_f I_f}{h_f^2} + \rho_b A_b \right)$$

$$H_3 = \left(\frac{\rho_f A_f (A2)^2}{4} + \frac{\rho_f I_f (A1)^2}{h_f^2} + \rho_t I_t + \rho_b I_b \right)$$

$$H_4 = \left(\frac{\rho_f A_f}{4} - \frac{\rho_f I_f}{h_f^2} \right),$$

$$H_5 = \left(\frac{\rho_f A_f (A2)}{4} + \frac{\rho_f I_f (A1)}{h_f^2} \right)$$

$$H_6 = \left(\frac{\rho_f A_f (A2)}{4} - \frac{\rho_f I_f (A1)}{h_f^2} \right)$$

$$H_7 = (\rho_t A_t + \rho_f A_f + \rho_b A_b)$$

$$Q_{33}^c = c_{33} - c_{13}^2 / c_{11}$$

$$Q_{55} = c_{55}$$

$$A_1 = (h_t + h_b) / 2,$$

$$A_2 = (h_t - h_b) / 2$$

$$A_3 = (h_t + 2h_c + h_b) / 2,$$

■ : denotes first derivative with respect to time (t) i.e., time derivative ($\partial/\partial t$)

■': denotes first derivative with respect to x i.e., spatial derivative

■'': denotes second derivative with respect to (x).

Appendix 2

$$[K_m] = \int_0^L [(N_t')B1(N_t') + (N_b')B2(N_b') + (N_w'')B3(N_w'') - (N_t')B4(N_b') - (N_b')B4(N_t') \\ + (N_t')B5(N_w'') + (N_w'')B5(N_t') + (N_b')B6(N_w'') + (N_w'')B6(N_b') \\ + N_t B7 N_t + N_b B7 N_b + (N_w')B8(N_w') + (N_t)B9 N_b + N_b B9 N_t \\ - N_b B10(N_w') - (N_w')B10 N_b + N_t B10(N_w') + (N_w')B10 N_t] dx$$

$$[K_{me}^a] = \int_0^L [(N_t)B11(V_c) - (N_b)B11(V_c) + (N_w')B12(V_c)] dx$$

$$[K_{em}^a] = \int_0^L (V_c)B11(N_t) - (V_c)B11(N_b) + (V_c)B12(N_w') dx$$

$$[K_e^a] = - \int_0^L (V_c)B13(V_c) dx$$